

Osteoporosis detection using convolutional neural network based on dual-energy X-ray absorptiometry images

Abulkareem Z. Mohammed¹, Loay E. George²

¹Department of Computer Science, Informatics Institute for Postgraduate Studies, Baghdad, Iraq

²Assistant of UoITc President for Scientific Affairs, University of Information Technology and Communication (UoITc), Baghdad, Iraq

Article Info

Article history:

Received Aug 7, 2022

Revised Sep 13, 2022

Accepted Sep 30, 2022

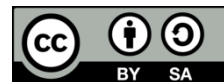
Keywords:

Bone mineral density
Convolutional neural network
Dual energy X-ray
absorptiometry
Osteoporosis
Spine

ABSTRACT

Osteoporosis is one of the most common diseases that affect the bones of adults, especially women in menopause, and the reason for this is due to the lack of bone mineral density bone mineral density (BMD). BMD can be measured by X-ray and dual energy X-ray absorptiometry (DEXA) images, this article, focused on using DEXA images for Osteoporosis detection. At first, the original image must passed through the preprocessing stage, during which the noisy parts is reduced, and the useless parts are eliminated, and then the contrast between adjacent areas is increased and the area of interest is allocated. After that, the image is passed in a deep learning model in order to extract the unique features on the basis of which each image is classified. The classification result was excellent with 98% accuracy. The used dataset is "Osteoporosis DEXA scans images" of Spine from Pakistan.

This is an open access article under the [CC BY-SA](https://creativecommons.org/licenses/by-sa/4.0/) license.



Corresponding Author:

Abulkareem Z. Mohammed

Department of Computer Science, Informatics Institute for Postgraduate Studies

Baghdad, Iraq

Email: phd202010550@iips.icci.edu.iq

1. INTRODUCTION

Osteoporosis the high rate of bone mineral loss causes a disease called Osteoporosis [1], [2] which is one of the most common causes of bone fracture [3], [4]. Especially in women in menopause [5], [6], as well as women who breastfeed children. Which leads to a lack of calcium in the women body, which decreases due to the frequent intake of medications, poor nutrition [7], drugs, and lack of exposure to sunlight [8]. It plays a role in increasing vitamin D3 which is responsible for fixing calcium in the body. All of these factors lead to significant reduction in bone structure [9]-[11]. In order to diagnose bone, whether it is infected or not, we need to measure bone mineral density [12], [13], there are several techniques to measure bone mineral density, such as X-ray [14], CT scan [15], dual energy X-ray absorptiometry (DEXA) [16] scan which differ in their quality and radiation dose. We will use DEXA because it has lower radiation dose than CT scan [17].

Lu *et al.* [18], showed a noise reduction algorithm for medical images, where he employed multi resolution analysis (MRA) and component substitution (CS). He calculated the threshold through CS after it was filtered. Then the bivariate threshold is used on the wavelet coefficients, where the image is processed, the last stage is to convert the result in reverse. The author compared Bayes' and other methods with the proposed system. Pal and Anburajan [19], presented an Osteoporosis detection via plain digital radiograph of calcaneus, using canny edge detection and get the number of black and white pixels when they calculated trabeculae of calcaneus. Gray level co-occurrence matrix (GLCM), is a texture analysis technique that was used to extract features. Bone mineral density determined by DEXA in the right proximal femur. Lu *et al.* [20], have introduced semi-supervised machine learning trained for DXA, using questionnaire data for Osteoporosis risk assessment. The model in this paper achieves the accuracy of 0.78. Agarwal *et al.* [21], the author employed a pre-trained

model from the CNN Alex net, taking into account the size of the image in proportion to the Alex net, and the accuracy was 96%. The author obtained a binary image from a grayscale one via thresholding, which step produced greater brightness and contrast than previously. Fathima *et al.* [22], showed how Osteoporosis can be diagnosed by bone mineral density (BMD), and how BMD can be measured by X-ray, DEXA, where the author showed that when using two types of images DEXSIT and XSITRAY. Then, they improved and enhanced the original images and divided the enhanced image and then the author employs deep learning and machine learning to get good finding.

Krishnaraj *et al.* [23], used deep learning to analyze sagittal view of CT spine, also used two U-nets for multiclass segmentation. The results of the paper showed that the specificity, accuracy and sensitivity of Osteoporosis detection is as follows 72.7 specificity, 82% accuracy, 84.4% sensitivity. Chen and Prasath [24] presented a new parameter for connectivity between the components to assess bone mineral density and (Z, T) score. Then, the scale value that defines connectivity between the components is evaluated. The value calculate both T, Z values that identify intensity value and quality. Hussain *et al.* [25], compare the current pixel label decision tree to the global threshold (GT), the region growing threshold (RGT), and artificial neural network (ANN). On a DXA picture, the segmentation accuracy was 91.4% greater.

2. PROPOSED SYSTEM

Figure 1 shows the developed system for Osteoporosis detection. It is consists of 4 stages: i) image loading from dataset, ii) pre-processing Which prepares the image in an appropriate manner, eliminating noise, correction, and extracting the area of interest, followed by iii) Smudging to obtain agglomerations with close values Which contributed to raising the accuracy of iv) Osteoporosis detection model convolutional neural network (CNN). Methods section will explain each stage in detail.

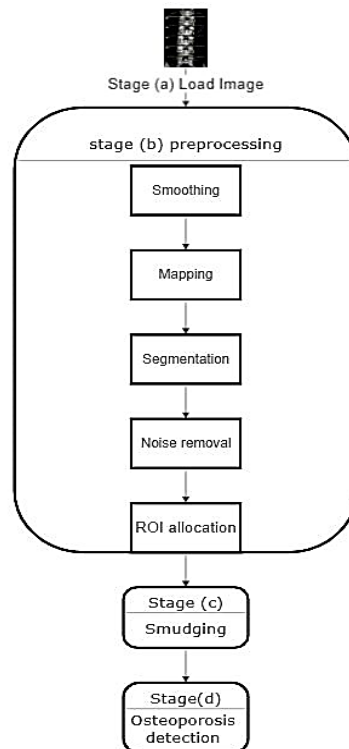


Figure 1. The layout of the developed system for Osteoporosis detection

3. METHODS

As we explained earlier, the proposed system contains several basic stages: first stage is loading original image from dataset. second stage is preprocessing stage. Followed by smudging stage. Finally, classification using convolutional neural network. All these stages will be discussed in details stages that will discuss in detail in this section.

3.1. Pre-processing

The original image contains many uninformative parts, it is preferable to remove these elements and properly prepare the image before diagnosing it because the original image has a lot of uninformative portions. Which in turn reduces the accuracy of the diagnosis: this procedure is known as pre-processing. This stage consists of several secondary stages through which the image is prepared correctly to be classified.

3.1.1. Smoothing

The acquired image will be noisy because of the low radiation dose we used to obtain it, so we improve it by applying a smoothing filter. The (3×3) mean filter was used for this task. The original and smoothed images are shown in Figures 2 and 3.

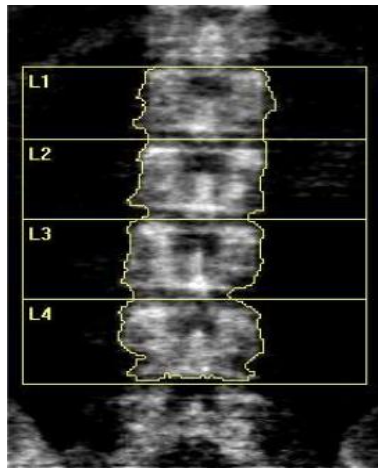


Figure 2. Original image DEXA image

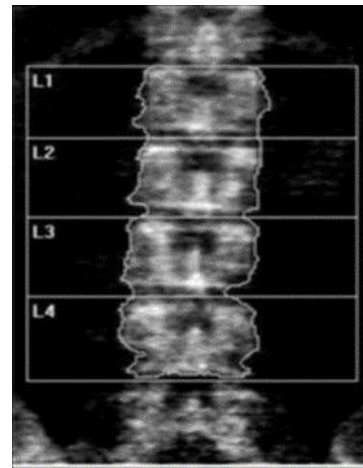


Figure 3. Smoothed image using mean Filter

3.1.2. Mapping

Gamma mapping presents to correct bright and dark region as needed according to (1).

$$G_{out} = \left(\frac{G_{in} - Min}{Max - Min} \right)^\gamma * 255 \tag{1}$$

When γ greater than 1, the contrast of the light gray area is enhanced. When γ smaller than 1, the contrast of the dark gray area is enhanced. When $\gamma=1$, this transformation is linear, that is, the original image is not change. Figure 4 shows Gamma mapping progress. Figure 5 shows gamma mapping result with $\gamma=2$.

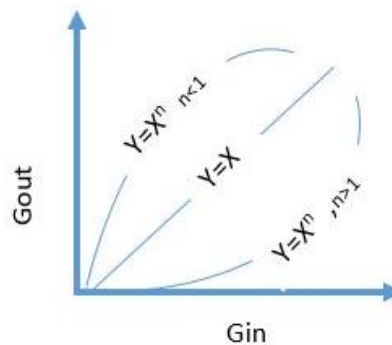


Figure 4. G-mapping for correcting images

3.1.3. Segmentation

In order to region of interest allocation there is a need to separate image background from object using what is known segmentation process, which isolate spine from background based on variable threshold

according to local pixel value. The main objective of segmentation is to facilitate the subsequent steps of pre-processing. Figure 6 presents the segmented image.

3.1.4. Noise removal

It is the process of removing distorted pixels spread over background of an image using via line mask erosion. Erosion is one of the most important morphology operations, which aims to extend the background and reduce the foreground, by sliding the structure element over the whole image. When the center pixel and all its neighbor have value (1) the background is set to be object (foreground), if any of the pixel value is (0) it remains background as shown in Figure 7.

3.1.5. Region of interest (ROI)

Because raw images have a lot of uninformative areas that slow down processing and reduce accuracy. It is important to crop them into areas that have the rich information needed to represent the entire image. I.e. a portion of the image required to operate on the image. When attempting to identify which class an image belongs to, ROI saves both time and effort as shown in Figure 8.

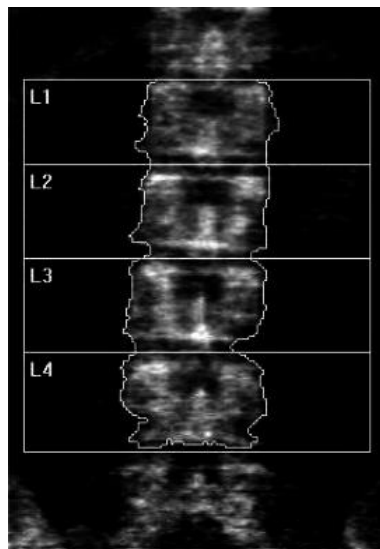


Figure 5. Corrected image by G-mapping



Figure 6. Segmented image

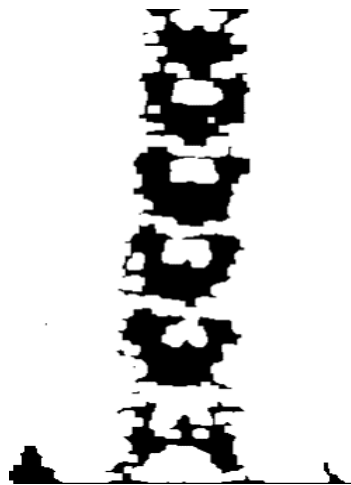


Figure 7. Noise removal by erosion



Figure 8. ROI allocation

3.2. Smudging

It is the process of merging small scattered and converging areas and converting them into agglomerations. All the pixels in one agglomerations have close values, and agglomerations differ in size and color. This technique is used in remote sensing where small details are neglected and make the region has one color to better understand the map, where the agricultural areas are given a green color even if they are separate, while the water is colored blue or cyan. The same can applies to medical images, where small, useless details are neglected. The result is an image that is easy to classify, as shown in Figure 9.



Figure 9. Smudging using mean filter [7x7, 5x5 and 3x3 window size]

3.3. Classification using convolutional neural network

The pre-processed image is being ready for feature extraction, matching, and decision. The proposed system shortens these steps by using the convolutional neural network (CNN) which consists of a number of layers. Table 1 shows all layers with their parameters.

Table 1. CNN model

Layer	Param
imageInputLayer	[400 90 3]
convolution2dLayer	(3,9,'Padding','same')
batchNormalizationLayer	default
reluLayer	default
maxPooling2dLayer	(2,'Stride',2)
convolution2dLayer	(3,27,'Padding','same')
batchNormalizationLayer	default
reluLayer	default
maxPooling2dLayer	(2,'Stride',2)
convolution2dLayer	(3,81,'Padding','same')
batchNormalizationLayer	default
reluLayer	default
dropoutLayer	(0.5)
fullyConnectedLayer	(3)
softmaxLayer	
classificationLayer	

- a. Convolutional layer: This layer extracts features by sliding a weighted mask over the source image and performing dot product multiplication to create a feature map. The weights are produced at random after going through the batch normalization (BN), pooling, and rectified linear unit (ReLU) layers several times. Weights that represent features are adjusted until they are optimal for the input image.
- b. Batch normalization (BN): A large number of each channel is reduced by the batch normalization (BN) layer by first normalizing the activation of each channel by subtracting the mean of the mini-batch and dividing on the standard deviation of the mini-batch, and then shifting and scaling the input of the layer. By doing this, the training process is sped up and network startup sensitivity is eliminated. This layer is used in between the convolutional layer and the ReLU layer.

- c. Rectified linear unit (ReLU): Since images are inherently non-linear and contain non-linear elements like color and border, the rectifier function is used to enhance the non-linearity of the image. In order to guarantee that just the robust feature was selected, ReLU was used to change all negative integers to zero and only use positive values. ReLU is one of best layers the used to increase non-linearity.
- d. Max pooling layer: The use of a max pooling layer has reduced spatial pattern. Important features are returned by sliding a mask with a known dimension over the feature map produced by the previous convolutional layer, but the max is empty. At each step, the highest value lying beneath this mask is chosen for the new feature map, which is then passed to the subsequent convolutional layer.
- e. Fully connected layer: This layer represents a feature vector that contains the most crucial data from the input; during training. It collects the features from all prior convolutional layers that can be used for identification later. For example, it trains a hidden layer to provide the likelihood of each class.
- f. SoftMax layer: Each class has a probability. For example (0.01, 0.9). The output of the softMax layer is a probability number ranging from zero to one (0-1). (0.011, 0.005). Softmax gives the candidate class a high probability and ignores the others.
- g. Loss of function: This function is used to calculate the loss (error) at each trading epoch. It is also a significant factor that is crucial to the backpropagation updating of weight. It illustrates the discrepancy between the genuine label and the expected output.

4. RESULTS AND DISCUSSION

The results showed that the smudging process increased the accuracy of the diagnosis by an excellent rate where the accuracy of detection on the original image without preprocessing 46% and after preprocessing was 78%, while when using smudging the results reached 98%. Where the CNN deep learning algorithm was used and the parameters were 100 epoch, learning rate 0.01. The dataset was divided between training and testing 75% and 25% respectively. It is worth noting that the number of samples used for each class is 54 samples.

5. CONCLUSIONS

The study showed that the use of the original dataset images could not be relied upon in the diagnosis unless it went through preprocessing step. The study also showed that the process of removing noise, correcting the image using Gamma and truncation of the region of interest will increase the accuracy of the detection and reduce the processing and training time. Finally, the results of the study showed that the smudging process has increased the accuracy of the diagnosis to some extent, and that the use of the CNN model is better than the traditional methods as it extracts the features automatically instead of relying on a single feature and this saves time and effort.




REFERENCES

- [1] J. A. Kanis, P. Delmas, P. Burckhardt, C. Cooper, and D. O. Torgerson, "Guidelines for diagnosis and management of osteoporosis," *Osteoporosis international*, vol. 7, no. 4, pp. 390–406, 1997, doi.org/10.1007/BF01623782.
- [2] M. Elemmi, G. Hugar, and S. Kallur, "Recognition of Osteoporosis through CT-images," *International Journal of Advanced Research in Computer and Communication Engineering*, vol. 4, 2015.
- [3] S. M. N. Fathima, R. Tamilselvi, and M. P. Beham, "A survey on Osteoporosis detection methods with a focus on X-ray and DEXA images," *IETE J Res*, pp. 1–25, 2020, doi: 10.1080/03772063.2020.1803771.
- [4] M. A. Al-antari *et al.*, "Non-local means filter denoising for DEXA images," in *2017 39th Annual International Conference of the IEEE Engineering in Medicine and Biology Society (EMBC)*, 2017, pp. 572–575, doi: 10.1109/EMBC.2017.8036889.
- [5] N. Li, X. Li, L. Xu, W. Sun, X. Cheng, and W. Tian, "Comparison of QCT and DXA: Osteoporosis detection rates in postmenopausal women," *Int J Endocrinol*, 2013, doi: 10.1155/2013/895474.
- [6] R. Lorente-Ramos, J. Azpeitia-Armán, A. Muñoz-Hernández, J. M. García-Gómez, P. Díez-Martínez, and M. Grande-Bárez, "Dual-energy X-ray absorptiometry in the diagnosis of Osteoporosis: a practical guide," *AJR-American Journal of Roentgenology*, vol. 196, no. 4, p. 897, 2011, doi:10.2214/AJR.10.5416.
- [7] S. K. Papadopoulou *et al.*, "Exercise and nutrition impact on Osteoporosis and sarcopenia—the incidence of osteosarcopenia: A narrative review," *Nutrients*, vol. 13, no. 12, p. 4499, 2021, doi: 10.3390/nu13124499.
- [8] T. Sözen, L. Özişik, and N. Ç. Başaran, "An overview and management of Osteoporosis," *Eur J Rheumatol*, vol. 4, no. 1, p. 46, 2017, doi: 10.5152/eurjrheum.2016.048.
- [9] V. A. Buzanovskii, "Determination of calcium in blood," *Rev J Chem*, vol. 9, no. 1, pp. 12–70, 2019, doi: 10.1134/S2079978018040027.
- [10] S. A. Razavi, "Calcium determination in EDTA treated plasma by colorimetric method and microplate reading format," 2015.
- [11] J. A. Kanis *et al.*, "SCOPE 2021: a new scorecard for Osteoporosis in Europe," *Arch Osteoporosis*, vol. 16, no. 1, pp. 1–82, 2021, doi: 10.1007/s11657-020-00871-9.
- [12] K. G. Faulkner, E. V. Stetten, and P. Miller, "Discordance in patient classification using T-scores," *Journal of Clinical Densitometry*, vol. 2, no. 3, pp. 343–350, 1999, doi: 10.1385/JCD:2:3:343.




- [13] E. W. Yu, B. J. Thomas, J. K. Brown, and J. S. Finkelstein, "Simulated increases in body fat and errors in bone mineral density measurements by DXA and QCT," *Journal of bone and mineral research*, vol. 27, no. 1, pp. 119–124, 2012, doi: 10.1002/jbmr.506.
- [14] R. Dendere, J. H. Potgieter, S. Steiner, S. P. Whitley, and T. S. Douglas, "Dual-energy X-ray absorptiometry for measurement of phalangeal bone mineral density on a slot-scanning digital radiography system," *IEEE Trans Biomed Eng*, vol. 62, no. 12, pp. 2850–2859, 2015, doi: 10.1109/TBME.2015.2447575.
- [15] T. M. Link, "Osteoporosis imaging: state of the art and advanced imaging," *Radiology*, vol. 263, no. 1, p. 3, 2012, doi: 10.1148/radiol.12110462.
- [16] A. B. Shaikh, M. Sarim, S. K. Raffat, K. Ahsan, A. Nadeem, and M. Siddiq, "Artificial neural network: a tool for diagnosing Osteoporosis," *Res J Recent Sci ISSN*, vol. 2277, p. 2502, 2014.
- [17] D. Hussain, S.-M. Han, and T.-S. Kim, "Automatic hip geometric feature extraction in DXA imaging using regional random forest," *J Xray Sci Technol*, vol. 27, no. 2, pp. 207–236, 2019, doi: 10.3233/XST-180434.
- [18] J. Lu, L. Wang, Y. Li, and T. Yahagi, "Noise removal for medical x-ray images in multiwavelet domain," *Int J Image Graph*, vol. 8, no. 01, pp. 25–46, 2008, doi: 10.1142/S0219467808002952.
- [19] A. B. Pal and M. Anburajan, "Digital image processing of calcaneum X-ray in the evaluation of Osteoporosis in women: A comparison with DXA bone densitometer as a 'standard,'" in *Proceedings of the International conference on Electronics and Communication Systems*, 2016, pp. 1865–1869.
- [20] L. Lu, L. Tao, W. Yining, H. Jiahui, and L. Jianfeng, "Research on Osteoporosis risk assessment based on semi-supervised machine learning," in *Proceedings of the 2020 Artificial Intelligence and Complex Systems Conference*, 2020, pp. 114–120, doi: 10.1145/3407703.3407725.
- [21] A. Agarwal, K. Patni, and D. Rajeswari, "Lung cancer detection and classification based on alexnet CNN," in *2021 6th International Conference on Communication and Electronics Systems (ICCES)*, 2021, pp. 1390–1397, doi: 10.1109/ICCES51350.2021.9489033.
- [22] S. M. N. Fathima, R. Tamilselvi, M. P. Beham, and A. Nagaraj, "A deep learning approach on segmentation of bone for bmd measurement from dexa scan images," in *2020 Sixth International Conference on Bio Signals, Images, and Instrumentation (ICBSII)*, 2020, pp. 1–5, doi: 10.1109/ICBSII49132.2020.9167573.
- [23] A. Krishnaraj *et al.*, "Simulating dual-energy X-ray absorptiometry in CT using deep-learning segmentation cascade," *Journal of the American College of Radiology*, vol. 16, no. 10, pp. 1473–1479, 2019, doi: 10.1016/j.jacr.2019.02.033.
- [24] L. Chen and V. B. S. Prasath, "Measuring bone density connectivity using dual energy X-ray absorptiometry images," *International Journal of Fuzzy Logic and Intelligent Systems*, vol. 17, no. 4, pp. 235–244, 2017, doi: 10.5391/IJFIS.2017.17.4.235.
- [25] D. Hussain, M. A. Al-Antari, M. A. Al-Masni, S.-M. Han, and T.-S. Kim, "Femur segmentation in DXA imaging using a machine learning decision tree," *J Xray Sci Technol*, vol. 26, no. 5, pp. 727–746, 2018, doi: 10.3233/XST-180399.

BIOGRAPHIES OF AUTHORS



Abulkareem Z. Mohammed    PhD student, received the B.Sc. degree in computer science from the Al-anbar University, Iraq, the M.Sc. degree in computing from the Informatics institute for postgraduate studies, Iraq. He can be contacted at email: phd202010550@iips.icci.edu.iq or abulkareemzwin@gmail.com.



Loay E. George    Assistant Professor, PhD holder since 1979, a member of teaching staff in college of science/ Baghdad University, Iraq. Currently working as assistant of UoITc President for Scientific Affairs. His main research concerns are: Digital Multimedia Processing; Coding (encryption, digital signature, data compression, representation); Pattern Recognition and Classification; Fast Strings Processing and Analysis; Biometrics; and Visual Based application. Disciplines artificial intelligence information science computer graphics pattern recognition, digital image processing, image retrieval, biometrical designs computer programming, data compression, computer vision, medical and biomedical image processing, image compression, fractals digital watermarking, images fractal dimension image processing, signal, image and video processing, feature extraction, image data analysis. He can be contacted at email: loayedwar57@yahoo.com.